Pergamon

Solid State Communications, Vol. 90, No. 4, pp. 281–284, 1994
Elsevier Science Ltd

0038–1098/94 $6.00 + .00

0038–1098(94)E0032–7

PICOSECOND OPTICAL BISTABILITY OF ZnTe–ZnS STRAINED LAYER SUPERLATTICES GROWN ON TRANSPARENT SUBSTRATE BaF_2 BY MOCVD

Y.M. Lu, X.W. Fan, Z.P. Guan and B.J. Yang

Changchun Institute of Physics, Academia Sinica, Changchun 130021, People's Republic of China

(*Received* 24 *May* 1993; *in revised form* 25 *December* 1993 *by G. Fasol*)

ZnTe–ZnS strained-layer superlattices (SLSs) were grown on ⟨1 1 1⟩ oriented BaF_2 substrates by atmospheric pressure metalorganic chemical vapour deposition (MOCVD). The formation of the superlattice structure was confirmed by X-ray diffraction measurement. Optical bistability (OB) in ZnTe–ZnS SLSs has been observed at 300 K for the first time with ps switching time. The origin of the optical bistability was investigated by photoluminescence (PL) measurement. The OB is attributed to increasing absorption effect due to band-gap shrinkage of the superlattices in high-intensity photoexcitation.

1. INTRODUCTION

II–VI COMPOUND semiconductor strained-layer superlattices (SLSs) such as ZnSe–ZnS, ZnTe–ZnSe, ZnTe–ZnS etc. are thought to be promising materials for efficient optoelectronic devices working in the visible spectra region [1–3]. In these novel optoelectronic devices, OB in particular has received much attention. Shen and Fan *et al.* have studied the excitonic absorptive optical bistability [4] and excitonic dispersive optical bistability [5] at 77 K in ZnSe–ZnS multiple quantum wells. Recently, they [6] reported optical bistability in ZnTe–ZnSe SLSs at 300 K with ps response. ZnTe–ZnS SLSs are a large lattice mismatch SLSs system and have a lattice mismatch of nearly 12%. ZnTe–ZnS SLSs have been successfully grown with the help of advanced growth techniques, e.g. molecular beam epitaxy (MBE) [7], atomic layer epitaxy (ALE) [8] and hot wall epitaxy (HWE) [1]. We [9] have reported for the first time growth of ZnTe–ZnS SLSs on CaF_2(1 1 1), BaF_2(1 1 1) and GaAs(0 0 0) substrates by MOCVD at atmospheric pressure. In this paper, the optical bistability of ZnTe–ZnS SLSs grown on BaF_2 substrates was observed for the first time at 300 K. The mechanism was investigated by PL measurement.

2. EXPERIMENTAL

ZnTe–ZnS SLSs were growth on ⟨1 1 1⟩ BaF_2 substrates by using a conventional MOCVD apparatus. Dimethylzine (DMZn), diethyltellurium (DETe) and 10% H_2S together with H_2 gas were used as the source materials for zinc, tellurium and sulphur, respectively. High-purity H_2 was used as carrier gas. A ZnS buffer layer is intentionally inserted to avoid lattice mismatch between substrate and superlattice. The substrate temperatures were varied between 380 and 420°C to optimize the growth conditions. The growth rates were 18–40 nm min^{-1} for ZnTe and 10–30 nm min^{-1} for ZnS layers under different flow.

The bistable experiment was carried out with the 532 nm line of a Nd:YAG laser. The laser pulse was 400 ps in duration (FWHM). The laser pulse was transmitted to the sample through an optical delay device. The incident laser and transmitted signals were simultaneously detected by using a streak camera triggered by electrical delay signals. The time dependence of the incident I_0 and transmitted I_t pulses were displayed on the screen of a television monitor. The bistable experimental setup is shown in Fig. 1.

3. RESULTS AND DISCUSSION

A typical X-ray diffraction pattern from the ZnTe–ZnS SLSs on a ⟨1 1 1⟩ BaF_2 substrate measured by a conventional diffractometer using Cu $K\alpha$ lines is shown in Fig. 2. In addition to the $K\alpha_1$ and $K\alpha_2$(1 1 1) diffraction peaks of the BaF_2

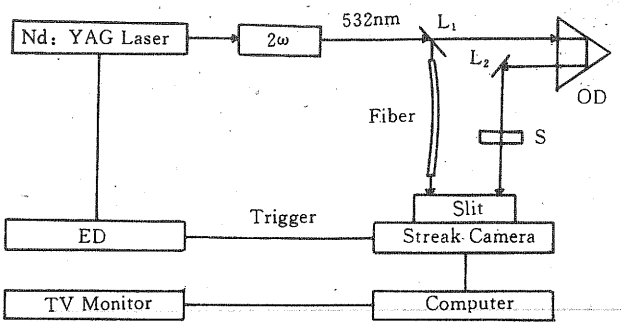

Fig. 1. Experimental apparatus for measuring optical bistability. 2ω: frequency multiplier, OD: optical delay device, L_1 and L_2: Lens, ED: electrical delay device.

substrates, some satellite peaks were observed. The superlattice structure was confirmed from this pattern. Figure 3 shows the bistable experimental result for the ZnTe–ZnS SLSs with 10 nm ZnS layers and 2 nm ZnTe layers at 300 K. Figure 3(a) and (c) give the time trace of the incident beam intensities I_0 and transmitted beam intensities I_t under low and high excitation densities. Figure 3(b) and (d) show the output intensities I_t as a function of the corresponding input intensities I_0 for two different excitation densities. It should be noticed from Fig. 3(a) that the shape of the transmitted pulse is unchanged compared with the shape of incident pulse when low excitation intensity pulse passed through the sample. The transmitted intensities I_t depends linearly on incident intensities I_0, as can be seen in Fig. 3(b). In Fig. 3(c), the shape of the transmitted pulse shows

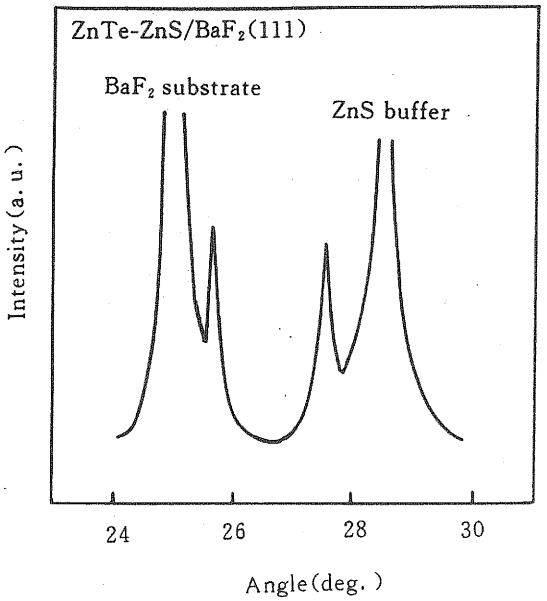

Fig. 2. X-ray diffraction profile of ZnTe–ZnS SLSs on (1 1 1) BaF_2 substrate.

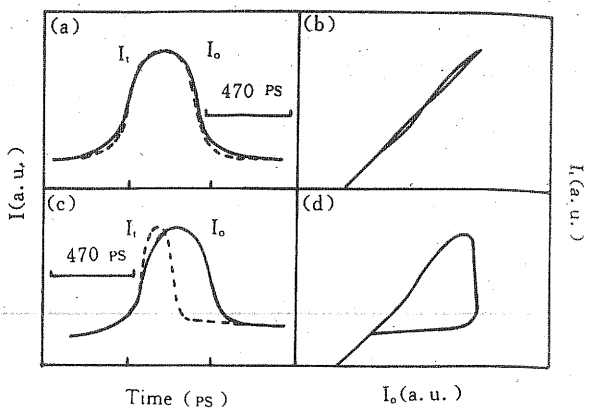

Fig. 3. Time dependence of incident (solid) I_0 and transmitted (broken) I_t pulses (a) and (c) in the ZnTe–ZnS/BaF_2 SLSs at 300 K and the resulting hysteresis loop (b) and (d). (a) and (b): low excitation intensity, (c) and (d): high excitation intensity.

a deformity compared to the shape of incident pulse under high excitation intensities. Figure 3(d) gives the corresponding hysteresis loops of the optical bistability.

We measured the PL spectra of the ZnTe (2 nm)–ZnS (10 nm) SLSs to investigate the origin of the optical bistability. The PL spectra of the sample at 77 K excited by the 337.1 nm line of a N_2 laser with a pulse width of 10 ns and frequency of 20 Hz, are presented in Fig. 4. It is obvious that the band has two peaks located at 510 nm and 540 nm, respectively. ZnTe–ZnS SLSs are predicted to be a type-II

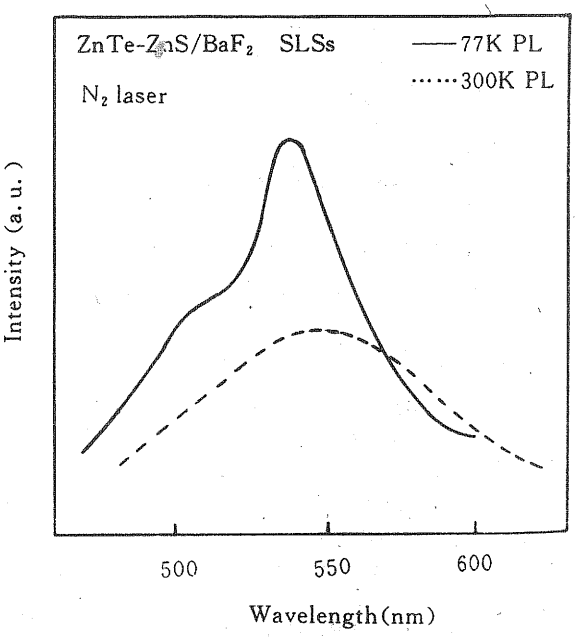

Fig. 4. PL spectra of ZnTe–ZnS/BaF_2 SLSs at 77 K (solid) and 300 K (broken), respectively. (Excited by the 337.1 nm line of a N_2 laser, $J_0 = 2\,\mathrm{MW\,cm^{-2}}$.)

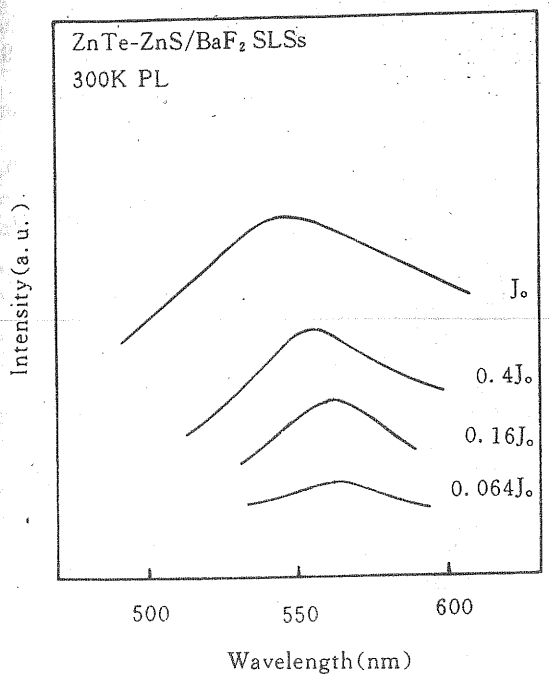

Fig. 5. PL spectra of ZnTe–ZnS/BaF_2 at 300 K at different excitation densities. (Excited by the 532 nm line of a Nd : YAG laser, $J_0 = 10\,MW\,cm^{-2}$.)

superlattice system consisting of electron-wells in the ZnS layer and hole-wells in the ZnTe layer. Theoretical calculation by using the Kronig–Penny model shows that the PL peak wavelength attributed to the quantized level emissions between $n = 1, 2$ electron subbands and $n = 1, 2$ heavy-hole subbands should be around 545 nm, 505 nm and 77 K. By fitting to experimental result, two peaks of the band observed in the PL spectra are considered to be free carrier recombination from $n = 1, 2$ electron subbands to $n = 1, 2$ heavy-hole subbands. The details about the origin of the band at 77 K have been published in [10]. In Fig. 4, we also gave the PL spectra of the same sample at 300 K by a N_2 laser excitation. It is noticed that a strong and rather broad emission is located at around 545 nm. Christen *et al.* [11] believed that the superlattice luminescence at 300 K should include a complicated process related to different subband recombinations and the intersubband transitions due to hot carrier exciting. At higher excess carrier densities, the recombination of subbands lying higher in energy is becoming increasingly important. The calculation shows the emissions between $n = 1, 2$ electron subbands and $n = 1, 2$ heavy-hole subbands should be around 570 and 530 nm at 300 K. In contrast the PL spectra (broken) in Fig. 4, we consider that the origin of the broad band is the composition of the above mentioned two recombination processes. Figure 5 shows the PL spectra of the above same sample at 300 K by 532 nm line of a Nd : YAG laser excitation with different densities. Under lower density excitation, the band peaks at 565 nm and has weaker intensity and narrower linewidth. With increasing excitation densities, this band peak shifts to the high-energy side, and the intensities increase and the full width at half maximum (FWHM) broadens, while for $J \sim J_0$, the band peak is located at around 540 nm. The photon energy of Nd : YAG laser is 2.331 eV (532 nm), the energy is not enough for exciting the transition from $n = 2$ electron subband to $n = 2$ heavy-hole subband. When the excitation density is strong enough, the effect of band-gap shrinkage [12] in the superlattices would be produced due to Coulomb interaction between free carriers, the photon energy could be resonant with the energy of $n = 2$ band-to-band transition related to heavy-hole. In Fig. 5, it is obvious that the low-energy tail is rapidly rising with increasing excitation intensity. Moreover, the high-energy side broadening of the band is also evident at. These results demonstrate the existence of band-gap shrinkage effect [12]. Under lower excitation density, the luminescence comes principally from recombination of $n = 1$ electrons to $n = 1$ heavy-hole. In high-intensity excitation, the recombination between $n = 2$ electron subband and $n = 2$ heavy-hole subband is becoming increasingly important due to band-gap shrinkage, and the luminescence peak shifts to high-energy side. The optical bistability could be explained by increasing absorption due to band-gap shrinkage in the superlattices. When high excitation intensity pulses pass through the sample, because of band-gap shrinkage in the superlattices, the resonant absorption would be formed by the quantum energy levels between $n = 2$ electrons and $n = 2$ heavy-holes with the photon energy of Nd : YAG laser. This leads to a rapid decrease of the transmitted beam intensity. So we may conclude that whether optical bistability is or is not observed at 300 K in high or low excitation intensities could be attributed to the increasing absorption effect due to band-gap shrinkage in the ZnTe–ZnS SLSs.

4. CONCLUSIONS

The ZnTe–ZnS SLSs have successfully been grown on BaF_2 substrates in atmospheric pressure MOCVD. We reported the first optical bistability of the ZnTe–ZnS SLSs at 300 K with ps switching time. By PL spectra measurement, we investigated the origin of the optical bistability. The bistable mechanisms are attributed to increasing absorption

effects due to band-gap shrinkage of the superlattices in high-intensity photoexcitation.

Acknowledgements — The authors would like to thank Z.S. Piao and K. Shi for the optical bistability measurements and M. Li and Z.J. Ge for the X-ray diffraction observation. This work is supported by the "863" High Technology Research Program in China and National Natural Science Foundation of China and Laboratory for Excited State Processes of Changchun Institute of Physics, Chinese Academy of Sciences.

REFERENCES

1. H. Fujiyasu, K. Mochizuki, Y. Yamazaki, M. Aoki, H. Kuwabara, Y. Nakanishi & G. Shimaoka, *Surf. Sci.* **174,** 543 (1986).
2. M. Kobayashi, N. Mino, M. Konagain & K. Takahashi, *Surf. Sci.* **174,** 550 (1986).
3. N. Teraguchi, Y. Takemura, R. Kimura, M. Konagai & K. Takahashi, *J. Crystal Growth* **93,** 720 (1988).
4. D.Z. Shen, X.W. Fan, G.H. Fan, L.C. Chen, C.F. Li & Y.D. Liu, *Acta Optica Sinica* **10,** 7 (1990).
5. D.Z. Shen, X.W. Fan, G.H. Fan & J.Y. Zhang, *J. Luminesc.* **48 & 49,** 299 (1991).
6. D.Z. Shen, X.W. Fan, Z.S. Piao & G.H. Fan, *J. Crystal Growth* **117,** 519 (1992).
7. T. Karasawa, K. Ohkawa & T. Mitsuyu, *J. Crystal Growth* **95,** 547 (1989).
8. T. Tckeda, T. Kuresu & M. Lida, *Surf. Sci.* **174,** 548 (1986).
9. Z.P. Gusn, Y.M. Lu, B.J. Yang & X.W. Fan, *Superlattices and Microstructures* **13,** 101 (1993).
10. Y.M. Lu, L.C. Chen, Z.P. Guan, A.H. Yang & X.W. Fan, *J. Infrared Millim. Waves* **12,** 159 (1993).
11. J. Christen & D. Bimberg, *Surf. Sci.* **174,** 261 (1986).
12. A. Cingolani, M. Ferrara & M. Lngara, *Phys. Rev.* **B19,** 4149 (1979).